# Performance Characteristics of a Concentric Annular Heat Pipe: Part II—Vapor Flow Analysis

**A. Faghri**
Professor,
Mechanical Systems Engineering,
Wright State University,
Dayton, OH 45435

*The solutions of the equations of fluid motion for compressible and incompressible flow in a concentric annular heat pipe have been analyzed. In addition, a similarity solution is presented that can predict the pressure losses in all the segments of the concentric annular heat pipe as well as conventional heat pipes. A theoretical analysis to predict the sonic limit for this new heat pipe is also presented.*

## Introduction

The analysis of heat pipes can be classified into the solutions of three fluid mechanics problems: (1) the pressure loss associated with the vapor flow in the evaporator, adiabatic, and condenser sections, (2) the pressure loss due to the liquid flow return path in the wick, and (3) the interaction between the liquid and vapor flows. The analysis for the last two problems is basically similar for different heat pipe structures but the dynamics of vapor flow is more complex due to the geometry and boundary specifications for nonconventional heat pipes. This is especially true for the performance analysis of the concentric annular heat pipe, which is shown in Fig. 1. In determining the heat capacity transmitted through this heat pipe, it is necessary to know the pressure losses in the separate segments of the heat pipe. The compressible vapor flow analysis is also needed for the sonic limit.

Many investigators have examined the problem of vapor flow in porous pipes and conventional heat pipes using numerical and analytical methods. The analysis of these theoretical and experimental investigations shows that approximate solutions of the Navier–Stokes equations using similarity analysis over the length of the condenser region for conventional heat pipes is valid for radial Reynolds numbers ranging from $0 < \mathrm{Re} < 2.3$ and $\mathrm{Re} > 9.1$ (Yuan and Findelstein, 1955; Bankston and Smith, 1973). In contrast to the condenser section, similarity solutions have been found to exist for all values of the radial Reynolds number in the evaporator section. Numerical solutions of the complete governing equations of motion for conventional heat pipes were also considered by Bankston and Smith (1973), Tien and Rohani (1974), and Busse and Prenger (1984). However, there is a disagreement among the investigators (Tien and Rohani, 1974; Busse and Prenger, 1984) on the validity of the usage of the parabolic version of the equations of motion to predict the vapor pressure drop in conventional heat pipes.

Faghri (1986) analyzed the two-dimensional, steady, and incompressible flow of vapor in a concentric annular heat pipe. The parabolic presentation of the governing equations of motion was used for the solution of the vapor flow in the evaporator, adiabatic, and condenser segments of the heat pipe. The solutions for the evaporator, adiabatic, and condenser sections were obtained independently of each other. This was possible by assuming a zero inlet axial velocity at the evaporator inlet and a fully developed profile at the inlet of the adiabatic and condenser sections. Due to these assumptions, an implicit marching finite-difference method was possible. Numerical solutions of the complete Navier–Stokes equations were also presented by Faghri and Parvani (1988) in order to allow for all of the features of laminar flow, especially in the condenser section in a problem that was clearly of the elliptic type.

This paper is a summary of the methods used for the calculation of the pressure drops in the different heat pipe segments and a theoretical investigation of the characteristics of the concentric annular heat pipe at low, moderate, and high-temperature applications. Because of the limitations of the previous studies for incompressible flow, a one-dimensional analysis of compressible vapor flowing within the evaporator and adiabatic sections of a concentric annular heat pipe, including the effect of friction, is also given for the calculation of the sonic limit. Practical and accurate equations for the calculation of the pressure losses are given that can be applied to concentric annular heat pipes as well as conventional heat pipes.

## Compressible Flow: One-Dimensional Analysis

The parameters limiting heat transport in conventional heat pipes are capillary limitations, sonic effects, entrainment, and boiling limitations. The type of limitation restricting the heat transport capability is determined by the temperature range under consideration, the working fluid, the wick structure, and the dimensions of the heat pipe. It is believed that the sonic limitation is not greatly influenced by any aspect of the wick structure except the vapor core size. Therefore, the choking phenomena should be of primary interest in the concentric annular heat pipe due to the fact that the vapor velocity becomes large and significant compared to the vapor sonic velocity. There have been many different vapor models proposed to analyze the gas dynamics choking phenomena in conventional heat pipes. Theoretical and experimental treatments of the sonic limitation have been made in the early stages of heat pipe development by Levy (1968, 1971), Kemme (1969), and Deverall et al. (1970). In this type of analysis the inertial forces and the compressibility effects are the most important phe-

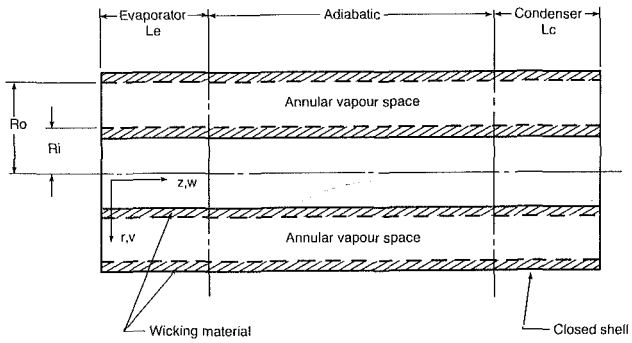


**Fig. 1 Concentric annular heat pipe and coordinate system**

Contributed by the Heat Transfer Division and presented at the National Heat Transfer Conference, Houston, Texas, July 1988. Manuscript received by the Heat Transfer Division May 4, 1988. Keywords: Heat Pipes and Thermosyphons.

nomena. The most recent prediction of the choking phenomenon in conventional heat pipes was done by Busse and Prenger (1984). They used the boundary layer approximation including the compressibility effects and predicted the choking phenomenon as a function of the radial Reynolds number. The analysis made here for concentric annular heat pipes is similar to those made by Levy (1968, 1971).

The analogy between the axial flow of vapor in the evaporator and the flow of a gas through a converging-diverging nozzle is well documented for conventional heat pipes. Similar to the analysis of conventional heat pipes, the flow in the vapor portion of the evaporator section of the concentric annular heat pipe can be thought of as annular flow between porous walls with mass injection at the walls. The following assumptions are made for the one-dimensional analysis of compressible vapor flow in the evaporator and adiabatic sections of the concentric annular heat pipe:

1 Frictional effects do not consider the effect of mass transfer.
2 The radial mass flow rate through the walls is uniform.
3 The radial distributions of the vapor temperature and pressure are neglected.

The principal of the conservation of mass, momentum, and energy as applied to a differential control volume element of length $dz$ in the annulus requires

$$A_v \frac{d}{dz}(\rho w) = \dot{m}_{I,E} + \dot{m}_{O,E} \tag{1}$$

$$\frac{dP}{dz} = -\frac{d(\rho w^2)}{dz} - \frac{4\bar{\tau}_w}{D_h} \tag{2}$$

$$\frac{d(h+w^2/2)}{dz} = -\frac{\dot{m}_{O,E}}{\dot{M}}\left(\frac{w^2}{2} - \frac{V_{O,E}^2}{2} + h - h_g\right) - \frac{\dot{m}_{I,E}}{\dot{M}}\left(\frac{w^2}{2} - \frac{V_{I,E}^2}{2} + h - h_g\right) \tag{3}$$

At this stage it is necessary to introduce some specific information on the vapor equation of state due to the compressibility flow analysis. Two different models have been used in the analysis of conventional heat pipes. These are the perfect gas and the equilibrium two-phase models. The equilibrium two-phase model is more realistic and therefore it has been used for the present analysis. The temperature and pressure are related by the Clausius-Clapeyron equation $dP/P = (h_{fg}/R)(dT/T^2)$ and the specific volume $v'$ and enthalpy $h$ are expressed in terms of the vapor quality $x$, the specific volume of saturated liquid and vapor, the enthalpy of the saturated liquid, and the latent heat of vaporization as done in the standard analysis of two-phase models. Upon using $v_g'$ as approximated by $RT/P$ and assuming that the specific volume of saturated liquid and liquid heat are constant quantities, the following relation is obtained for the axial pressure gradient:

$$\frac{dP}{dz} = \frac{\dfrac{w^2}{v'z}\left[2h_{fg} + \dfrac{(v_g'-v_f')}{v'}\left[w^2 - z\left\{\dfrac{\dot{m}_{O,E}}{\dot{M}}\left(\dfrac{w^2}{2} - \dfrac{V_{O,E}^2}{2} + h - h_g\right) + \dfrac{\dot{m}_{I,E}}{\dot{M}}\left(\dfrac{w^2}{2} - \dfrac{V_{I,E}^2}{2} + h - h_g\right)\right\}\right]\right] + F}{\left[-\left(h_{fg} + \dfrac{(v_g'-v_f')}{v'}w^2\right) + \dfrac{xw^2v_g'}{Pv'^2}\left(1 - \dfrac{RT}{h_{fg}}\right)h_{fg} + \dfrac{C_{pf}T^2w^2(v_g'-v_f')R}{h_{fg}Pv'^2}\right]} \tag{4a}$$

where $F = \dfrac{4\bar{\tau}_w}{D_h}\left(h_{fg} + \dfrac{w^2(v_g'-v_f')}{v'}\right)$.

The axial quality and velocity gradients are

$$\frac{dx}{dz} = \frac{\left[-1 + \left(1 - \dfrac{RT}{h_{fg}}\right)\dfrac{xw^2v_g'}{Pv'^2}\right]\dfrac{dP}{dz} - \dfrac{2w^2}{zv'} - \dfrac{4\bar{\tau}_w}{D_h}}{\left(\dfrac{v_g'-v_f'}{v'^2}\right)w^2} \tag{5a}$$

and

$$\frac{dw}{dz} = \frac{w}{z} + \frac{wxv_g'}{v'P}\left(\frac{RT}{h_{fg}} - 1\right)\frac{dP}{dz} + w\left(\frac{v_g'-v_f'}{v'}\right)\frac{dx}{dz} \tag{6a}$$

For both the inner and outer walls, the mass injection rates were taken to be uniform over the length of the evaporator section and are related to the axial mass flow rate $\dot{M}$ and the inner and outer local heat rate per unit length of the evaporator by the following relations:

$$\dot{M} = (\dot{m}_{I,E} + \dot{m}_{O,E})z \tag{7}$$

## Nomenclature

$A'$ = constant used in equation (26) = $(1-K^2)/\ln 1/K$
$A_v$ = cross-sectional area of the vapor flow passage
$B$ = constant used in defining $C$ = $(1-K^4)/(1-K^2)$
$C$ = constant used in equation (26) = $4(|\mathrm{Re}_{I,E}| + |\mathrm{Re}_{O,E}|)/(B-A')(1-K^2)$
$C'$ = constant used in equation (28) = $4(|\mathrm{Re}_{I,C}| + |\mathrm{Re}_{O,C}|)/(B-A')(1-K^2)$
$C_{pf}$ = constant pressure specific heat of liquid
$dz$ = increment in the $z$ direction
$D'$ = constant used in equation (28) = $2/(B-A')$
$D_h$ = hydraulic diameter
$DI$ = inner pipe diameter
$DO$ = outer pipe diameter
$f$ = friction factor
$h$ = enthalpy of vapor
$h_{fg}$ = enthalpy of evaporation
$h_g$ = enthalpy of saturated vapor
$K$ = ratio of the inner radius to the outer radius
$K'$ = ratio of specific heats of vapor
$LA$ = length of the adiabatic section
$LC$ = length of the condenser section
$LE$ = length of the evaporator section
$LT$ = total length of the heat pipe
$\dot{m}$ = mass injection rate per unit length of evaporator
$\dot{M}$ = axial mass flow rate
M = vapor Mach number
$P$ = vapor pressure
$P^+$ = normalized pressure = $(P-P_e)/\rho(w_{A,m})^2$
$Q$ = heat transfer rate per unit length of evaporator
$Q_s$ = sonic heat rate
$r$ = radial coordinate
$R$ = gas constant
$R^+$ = normalized radial distance = $r/RO$
$RI$ = inner pipe radius
$RO$ = outer pipe radius
Re = radial Reynolds number
$\mathrm{Re}_{I,E}$ = inner wall radial Re in evaporator = $(RI)(V_{I,E})/\nu$
$\mathrm{Re}_{I,C}$ = inner wall radial Re in condenser = $(RI)(V_{I,C})/\nu$
$\mathrm{Re}_{O,E}$ = outer wall radial Re in evaporator = $(RO)(V_{O,E})/\nu$

$$Q_{O,E} = \dot{m}_{O,E}\left(h_{fg} + \frac{V_{O,E}^2}{2}\right) \tag{8}$$

$$Q_{I,E} = \dot{m}_{I,E}\left(h_{fg} + \frac{V_{I,E}^2}{2}\right) \tag{9}$$

The radial velocities at the inner and outer walls are calculated in terms of the inner and outer local heat rate per unit length by the following relations, since the second term in equations (8) and (9) is small compared to the first term in the right-hand side of the same equations:

$$V_{O,E} = \frac{Q_{O,E}}{\pi\, DO\, \rho_g\, h_{fg}} \tag{10}$$

$$V_{I,E} = \frac{Q_{I,E}}{\pi\, DI\, \rho_g\, h_{fg}} \tag{11}$$

The relation

$$f = \frac{\bar{\tau}_w}{\rho\, w^2/2} = \frac{C_1}{\mathrm{Re}_z} \tag{12}$$

was used to calculate the laminar shear stress in the evaporator and adiabatic segments, where the constant $C_1$ is obtained from Kays and Crawford (1980) in terms of $K$. The above equation neglects the effect of mass transfer on the friction coefficient. It has already been well documented that blowing reduces the friction coefficient and therefore the actual prediction of the numerical results should be expected to lie between the numerical results for no friction and the results with friction. Equations (4*a*)–(6*a*) reduce to the governing equations for conventional heat pipes if $Q_{I,E} = \dot{m}_{I,E} = V_{I,E} = 0$ and represent frictionless flow if $\bar{\tau}_w = 0$.

Expressions similar to equations (4*a*), (5*a*), and (6*a*) will be obtained for the adiabatic section. These relations for the adiabatic section cannot be obtained from the evaporator results using $\dot{m}_{I,E} = \dot{m}_{O,E} = 0$, because the inlet condition to the adiabatic section is different from that to the evaporator section and one is not able to use equation (7) for the adiabatic section. These relations for the axial pressure, quality, and velocity gradients for the adiabatic section are

$$\frac{dP}{dz} = \frac{\left(\frac{w^2(\nu_g' - \nu_f')}{\nu'} + h_{fg}\right)\frac{4\bar{\tau}_w}{D_h}}{\left[-\left(h_{fg} + \frac{(\nu_g' - \nu_f')}{\nu'}w^2\right) + \frac{xw^2\nu_g'}{P\nu'^2}\left(1 - \frac{RT}{h_{fg}}\right)h_{fg} + \frac{C_{pf}T^2w^2(\nu_g' - \nu_f')R}{h_{fg}P\nu'^2}\right]} \tag{4b}$$

$$\frac{dx}{dz} = \frac{\left[-1 + \left(1 - \frac{RT}{h_{fg}}\right)\frac{xw^2\nu_g'}{P\nu'^2}\right]\frac{dP}{dz} - \frac{4\bar{\tau}_w}{D_h}}{\left(\frac{\nu_g' - \nu_f'}{\nu'^2}\right)w^2} \tag{5b}$$

and

$$\frac{dw}{dz} = \frac{wx\nu_g'}{\nu' P}\left(\frac{RT}{h_{fg}} - 1\right)\frac{dP}{dz} + w\left(\frac{\nu_g' - \nu_f'}{\nu'}\right)\frac{dx}{dz} \tag{6b}$$

Equations (4*b*)–(6*b*) form a system of three simultaneous first-order ordinary differential equations that can be solved for $P$, $x$, and $w$ as functions of $z$ provided that $Q_{I,E}$ and $Q_{O,E}$ are specified. It should be noted that the temperature and pressure are related through the Clausius-Clapeyron equation. These equations are solved by digital computer using the Runge-Kutta integration scheme. In the upstream end of the evaporator for the initial conditions, the incompressible assumption was made to obtain the following linear relation for the velocity at the initial step:

$$w_i = \frac{4(V_{I,E}\, DI + V_{O,E}\, DO)}{DO^2 - DI^2}\, z_i \tag{13}$$

All of the calculations are started at the upstream end of the evaporator where the fluid is assumed to be saturated vapor ($x = 1$) at the operating temperature of 773 K. In order to obtain the sonic limit, a certain $Q_{I,E}$ and $Q_{O,E}$ were assumed and then increased step by step in an iteration process. The process was continued until the Mach number, $M = (w/\sqrt{K'RT})$, reached unity at the exit of the adiabatic section when considering the friction or reached unity at the exit of the evaporator section when friction is neglected. The thermophysical properties of sodium were obtained by Vargaftik (1975).

The calculations were made for three different cases for the same sodium heat pipe with outer and inner diameters of 0.0444 m and 0.0294 m, respectively, and with evaporator and adiabatic section lengths of 0.08 m and 0.04 m, respectively. The three cases are: (1) neglecting the effect of friction and no

## Nomenclature (cont.)

$\mathrm{Re}_{O,C}$ = outer wall radial Re in condenser = $(RO)(V_{O,C})/\nu$
$\mathrm{Re}_z$ = axial Reynolds number
$T$ = temperature
$v$ = radial component of the vapor velocity
$v^*$ = dimensionless radial velocity = $v\, RO/\nu$
$V_{I,E}$ = blowing velocity at inner wall in evaporator
$V_{I,C}$ = suction velocity at inner wall in condenser
$V_{O,E}$ = blowing velocity at outer wall in evaporator
$V_{O,C}$ = suction velocity at outer wall in condenser
$V_{I,w}$ = radial velocity at inner wall
$V_{O,w}$ = radial velocity at outer wall
$w$ = axial component of vapor velocity
$w_{A,m}$ = mean axial velocity in adiabatic section
$w_{z,m}$ = local mean axial velocity
$w_{z,m}^*$ = dimensionless local mean axial velocity = $w_{z,m}/w_{A,m}$
$W^+$ = normalized axial velocity = $w/w_{z,m}$
$w^*$ = dimensionless axial velocity = $w/w_{A,m}$
$x$ = vapor quality
$z$ = axial coordinate
$z^*$ = dimensionless axial coordinate = $z\nu/(w_{A,m})(RO^2)$
$\mu$ = fluid absolute viscosity
$\nu$ = kinematic viscosity
$\nu'$ = specific volume of vapor
$\nu_f'$ = specific volume of saturated liquid
$\nu_g'$ = specific volume of saturated vapor
$\rho$ = fluid density
$\rho_g$ = density of saturated vapor
$\bar{\tau}$ = mean shear stress

**Subscripts**

$A$ = adiabatic section
$C$ = condenser section
$e$ = entrance of evaporator section
$E$ = evaporator section
$I$ = inner wall
$i$ = initial step
$O$ = outer wall
$m$ = mixed-mean
$w$ = at the wall
$z$ = at any $z$ location

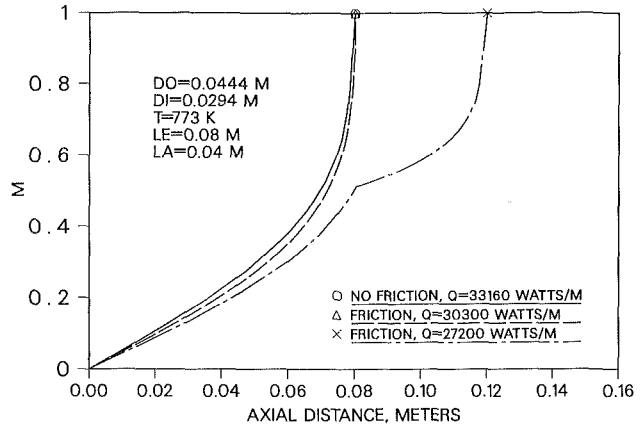


**Fig. 2 Mach number variation along the concentric annular heat pipe under symmetric heating at the occurrence of the sonic limit**

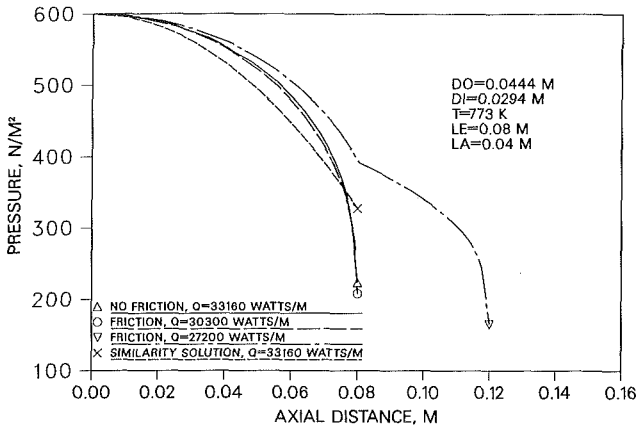


**Fig. 3 Pressure variation along the concentric annular heat pipe under symmetric heating at the occurrence of the sonic limit**

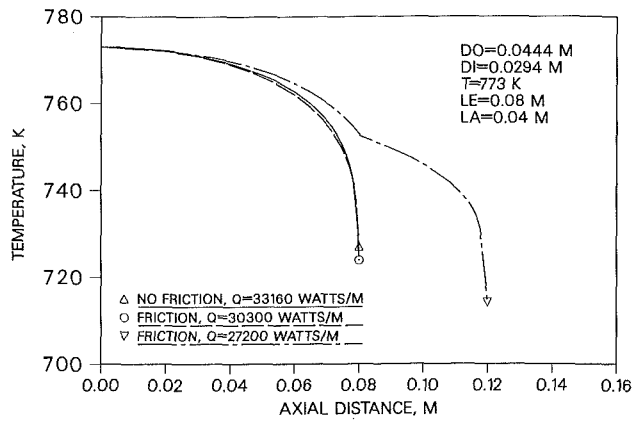


***Fig. 4 Temperature variation along the concentric annular heat pipe under symmetric heating at the occurrence of the sonic limit***

adiabatic section, (2) including the effect of friction and no adiabatic section, (3) including the effect of friction and having an adiabatic section. Figures 2–4 are graphs of the axial variation of the Mach number M, the static pressure $P$, and the temperature $T$, respectively, along the concentric annular heat pipe under a symmetric heating load when the sonic limit occurs. The infinite downstream gradients of M, $P$, and $T$ are another indication of the gas dynamics choking phenomenon predicted by the above analysis. When considering the effect of friction, the value of the critical sonic heat rate $Q_s$ = 15,150 W/m is smaller than the case neglecting friction ($Q_s$ = 16,580 W/m) by about 10 percent for this particular heat pipe and operating conditions. If there is an adiabatic section, the result will become even smaller ($Q_s$ = 13600 W/m) and the sonic limit will occur at the exit of the adiabatic section.

Using the simple perfect gas model, the following equation can be obtained for the sonic limit heat flux calculation for the annular heat pipe:

$$Q_s = \frac{\rho\sqrt{K'RT}\, h_{fg} \frac{\pi}{4}(DO^2 - DI^2)}{\sqrt{2(K+1)}} \tag{14}$$

where equation (14) is reduced to the equation given by Levy (1968) for $DI = 0$. The above equation underpredicts the actual numerical result presented in Figs. 2–4 for the case, which includes the effect of friction by 1/2 percent for the given operating conditions. Similar agreements were observed under asymmetric heating loads ($Q_{I,E} = 1/3\ Q_{O,E}$) with the same total heat load.

## Incompressible Flow: Two-Dimensional Analysis

The physical problem under consideration is a right circular cylindrical annular cavity as shown in Fig. 1. It is assumed that the vapor flow in all the segments of the concentric annular heat pipe—evaporator, adiabatic, and condenser sections—is operating under laminar, incompressible, steady conditions and the properties of the fluid are constant. The uniform radial inflow and outflow boundary conditions are modeling evaporation and condensation. Since the annulus is closed at both ends, it is required that the fluid that enters into the evaporator segment flow out through the condenser section. The differential equations associated with this axisymmetric problem are the continuity and the momentum equations as given below in cylindrical coordinates

$$\frac{\partial}{\partial z}(\rho w) + \frac{1}{r}\frac{\partial}{\partial r}(\rho r v) = 0 \tag{15}$$

$$w\frac{\partial}{\partial z}(\rho w) + v\frac{\partial}{\partial r}(\rho w) = -\frac{\partial P}{\partial z} + \mu\left[\left\{\frac{\partial^2 w}{\partial z^2}\right\} + \frac{1}{r}\frac{\partial w}{\partial r} + \frac{\partial^2 w}{\partial r^2}\right] \tag{16}$$

$$w\frac{\partial}{\partial z}(\rho v) + v\frac{\partial}{\partial r}(\rho v) = -\frac{\partial P}{\partial r} + \mu\left[\left\{\frac{\partial^2 v}{\partial z^2}\right\} + \frac{1}{r}\frac{\partial v}{\partial r} + \frac{\partial^2 v}{\partial r^2}\right] \tag{17}$$

It should be noted that in equations (16) and (17) the terms in braces are associated with axial diffusion terms. These terms are neglected when the parabolic version is considered but are accounted for in the elliptic case.

The boundary conditions are defined as follows:

$$\begin{aligned} w(0, r) &= v(0, r) = 0 \\ w(LT, r) &= v(LT, r) = 0 \\ w(z, RI) &= w(z, RO) = 0 \\ v(z, RI) &= V_{I,w}(z) \\ v(z, RO) &= V_{O,w}(z) \\ P\left(0, \frac{RI+RO}{2}\right) &= 0 \end{aligned} \tag{18}$$

The radial blowing and suction velocities at the inner and outer walls are taken to be uniform over the heating or cooling sections and are related to the local heat rate per unit length by the following relations:

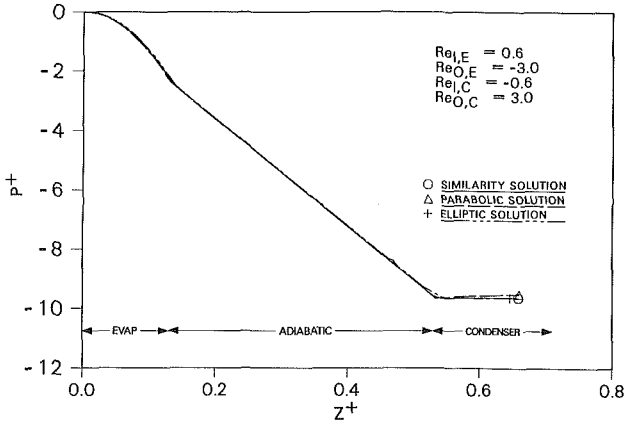


**Fig. 5 Comparison of elliptic, parabolic, and similarity analyses of the normalized pressure distribution along the concentric annular heat pipe for $K$ = 0.2 and low radial Reynolds numbers**

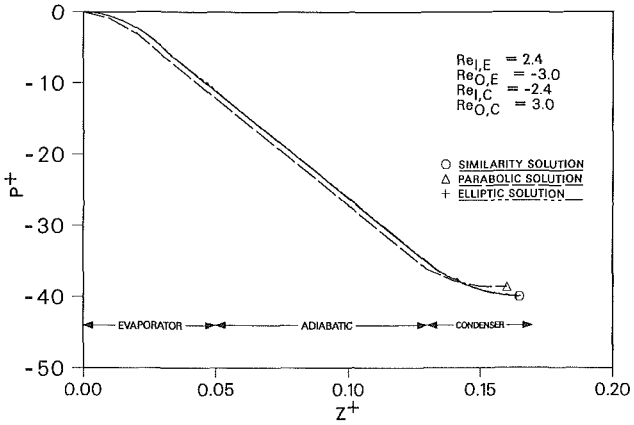


**Fig. 6 Comparison of the elliptic, parabolic, and similarity analyses of the normalized pressure distribution along the concentric annular heat pipe for $K$ = 0.8 for moderate radial Reynolds numbers**

$$V_{O,E} = \frac{Q_{O,E}}{\pi DO\rho h_{fg}}$$

$$V_{I,E} = \frac{Q_{I,E}}{\pi DI\rho h_{fg}}$$

$$V_{O,C} = \frac{Q_{O,C}}{\pi DO\rho h_{fg}}$$

$$V_{I,C} = \frac{Q_{I,C}}{\pi DI\rho h_{fg}}$$

The parabolic and elliptic presentations of the governing equations of fluid motion for steady two-dimensional laminar flow in a concentric annular heat pipe with various distributions of heating and cooling loads have been analyzed numerically. The results show that the flow reverses in long condenser segments or at very high condensation rates and the parabolic presentation provides a sufficiently accurate picture of the vapor pressure variations at both low and high evaporation and condensation rates.

In order to investigate the accuracy and reliability of the numerical results obtained from the boundary layer analysis (Faghri, 1986) with those obtained by the elliptic presentation of the governing equations, a comparison was made for two radius ratio $K$ values. Faghri (1986) employed the boundary layer approximation and analyzed the vapor flow in the evaporator and condenser sections independently. The elliptic analysis is accomplished by solving the vapor flow in the concentric annular heat pipe as one domain all along the heat pipe. The grid spacing in the present work was systematically varied and the results for different grid sizes were compared to the extrapolated results of an infinitesimal grid spacing. A mesh with 40 cells in the radial direction and 80 cells in the axial direction was used for all the results reported in this paper.

Figure 5 presents the normalized pressure distribution $P^+$ along the heat pipe for the case with $K$ = 0.2. The evaporator radial Reynolds numbers at the inner and outer walls are 0.6 and −3.0, respectively. The condenser radial Reynolds number at the inner wall is −0.6, while the radial Reynolds number at the outer wall is 3.0. The pressure drop results obtained from using the elliptic version of the governing equations are within 1 percent of those obtained by the boundary layer approximation.

Figure 6 presents the normalized pressure distribution $P^+$ for the case with $K$ = 0.8 and the radial Reynolds numbers at the inner wall in both the evaporator and condenser sections equal to 2.4. The radial Reynolds number at the outer wall in both the evaporator and condenser is set at 3.0. This case shows a deviation of 7 percent between the elliptic and parabolic presentations of the governing equations.

Figure 7 presents the normalized pressure variation for the case with $K$ = 0.65 and the evaporator and condenser radial Reynolds numbers of 1000 for both walls. The flow reversed for this particular case in the condenser section due to the very high condenser radial Reynolds numbers.

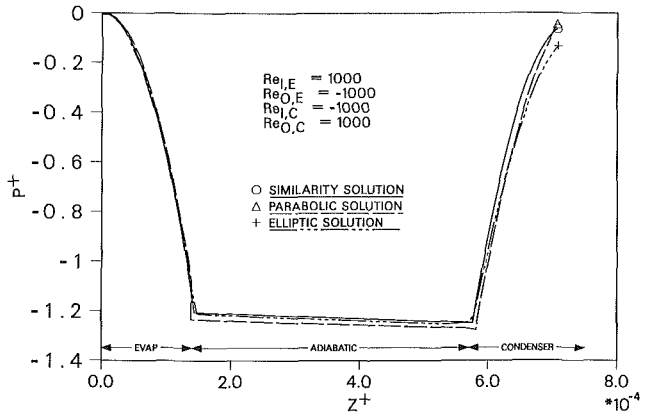


**Fig. 7 Comparison of the elliptic, parabolic, and similarity analyses of the normalized pressure distribution along the concentric annular heat pipe for $K$ = 0.65 and high radial Reynolds numbers**

## Incompressible Flow: Similarity Analysis

From the study by Faghri and Parvani (1988), one can generalize that the vapor flow in an annular heat pipe becomes fully developed in a very short distance from the evaporator end cap and this similar profile repeats itself in the adiabatic and condenser sections for low as well as moderate radial Reynolds numbers. This entry distance is not of significance in many practical applications. The criterion for a fully developed flow is that the normalized axial velocity $W^+ = w/w_{z,m}$ is invariant along the pipe. One very interesting feature of the numerical results given by Faghri and Parvani (1988) was that $W^+$ was similar for various radial Reynolds numbers including the case with zero inner and outer radial Reynolds numbers. The fully developed normalized velocity profile for annular flow for zero blowing velocity can be easily obtained analytically

$$W^+ = \frac{w}{w_{z,m}} = \frac{w^*}{w^*_{z,m}} = \frac{2\left[1 - R^{+2} + \left\{\frac{1-K^2}{\ln 1/K}\right\}\ln(R^+)\right]}{\left[\frac{1-K^4}{1-K^2} - \frac{1-K^2}{\ln 1/K}\right]} \quad (19)$$

The dimensionless local mean axial velocity $w^*_{z,m}$ can be obtained by making a mass balance in the evaporator section of the heat pipe

$$w^*_{z,m} = \frac{2(\mathrm{Re}_{I,E} + |\mathrm{Re}_{O,E}|)z^*}{1-K^2} \tag{20}$$

According to the numerical results, equation (19) also approximately presents the normalized velocity $W^+$ for all radial Reynolds numbers and $K$ values in the fully developed region.

Assuming that the fluid is incompressible, the normal radial velocity along the length of the pipe walls is constant, and the pressure along the radius of the pipe is constant, the system of equations in dimensionless form describing the vapor flow is reduced to the following form:

$$w^* \frac{\partial w^*}{\partial z^*} + v^* \frac{\partial w^*}{\partial R^+} = -\frac{\partial P^+}{\partial z^*} + \frac{1}{R^+}\frac{\partial}{\partial R^+}\left(R^+ \frac{\partial w^*}{\partial R^+}\right) \tag{21}$$

$$R^+ \frac{\partial w^*}{\partial z^*} + \frac{\partial (v^* R^+)}{\partial R^+} = 0 \tag{22}$$

The boundary conditions appropriate for the evaporator section are as follows:

$$\begin{aligned} v^*(R^+, 0) &= w^*(R^+, 0) = 0 \\ w^*(K, z^*) &= w^*(1, z^*) = 0 \\ v^*(K, z^*) &= \frac{RO\ V_{I,E}}{\nu} = \frac{\mathrm{Re}_{I,E}}{K} \\ v^*(1, z^*) &= \frac{RO\ V_{O,E}}{\nu} = \mathrm{Re}_{O,E} \end{aligned} \tag{23}$$

The system of equations of (21) and (22) is reduced to the following equation by elimination of the radial velocity in the evaporation section:

$$w^* \frac{\partial w^*}{\partial z^*} + \left[\frac{\mathrm{Re}_{I,E}}{R^+} - \frac{1}{R^+}\int_K^{R^+} R^+ \frac{\partial w^*}{\partial z^*} dR^+\right]\frac{\partial w^*}{\partial R^+} = -\frac{\partial P^+}{\partial z^*} + \frac{1}{R^+}\frac{\partial}{\partial R^+}\left(R^+ \frac{\partial w^*}{\partial R^+}\right) \tag{24}$$

The pressure drop is obtained by substituting expression (19) into the following integral equation:

$$\int_K^1 w^* \frac{\partial w^*}{\partial z^*} R^+ dR^+ - \int_K^1 \left[\frac{\partial w^*}{\partial R^+}\int_K^{R^+}\left(R^+ \frac{\partial w^*}{\partial z^*}\right) dR^+\right] dR^+ = -\frac{\partial P^+}{\partial z^*}\left(\frac{1}{2} - \frac{K^2}{2}\right) + \left(R^+ \frac{\partial w^*}{\partial R^+}\right)\Bigg|_K^1 \tag{25}$$

The pressure drop along the evaporator section of the concentric annular heat pipe is calculated using the following expression:

$$P^+_E = \frac{2}{K^2-1}\left[Cz^{*2}(1-K^2) + \frac{C^2 z^{*2}}{2}\left\{\frac{1}{3} - \frac{3}{4}A' + \frac{A'^2}{2} - K^2 + K^4 - 2A'K^2 \ln K + A'K^2 - \frac{K^6}{3} + A'K^4 \ln K - \frac{A'K^4}{4} - A'^2K^2(\ln K)^2 + A'^2K^2 \ln K - \frac{A'^2K^2}{2}\right\}\right] \tag{26}$$

A similar analysis can be made for the pressure drop in the condenser section by using the appropriate form for $w^*_{z,m}$ in equation (19). The following expression for $w^*_{z,m}$ is obtained by a mass balance in the condenser zone:

$$w^*_{z,m} = 1 - \frac{2(|\mathrm{Re}_{I,C}| + \mathrm{Re}_{O,C})z^*}{(1-K^2)} \tag{27}$$

The pressure drop in the condenser segment using the parabolic profile is given by

$$P^+_C = 4[(K^2 - 1 + C' \cdot E)/(K^2-1)][(C'z^{*2}/2) - D'z^*] \tag{28}$$

where $E$ is

$$E = \left\{\frac{1}{6} - \frac{3A'}{8} + \frac{A'^2}{4} - \frac{K^2}{2} + \frac{K^4}{2} - \frac{K^6}{6} - A'K^2 \ln K + \frac{A'K^2}{2} + \frac{(A'K^4 \ln K)}{2} - \frac{A'K^4}{8} - \frac{A'^2K^2(\ln K)^2}{2} + \frac{A'^2K^2 \ln K}{2} - \frac{A'^2K^2}{4}\right\} \tag{29}$$

It should be noted that equation (28) can be used to predict the pressure loss in the adiabatic segment by assuming $\mathrm{Re}_{I,C} = \mathrm{Re}_{O,C} = 0$

$$P^+_A = -4D'z^* \tag{30}$$

Figures 3, 5, 6, and 7 also demonstrate the normalized pressure distribution using the similarity analysis. The excellent agreement between the similarity analysis and the solution of the elliptic version of the governing equations indicates that the axial velocity profile becomes fully developed in a short distance and stays parabolic all along the length of the heat pipe for both cases. The flow did not reverse for the first two cases because the condenser zone is short and the radial Reynolds numbers are small. There is a region where the flow reverses in the condenser for case 3 because the radial Reynolds numbers are high (Faghri and Parvani, 1988). This demonstrates that the similarity results surprisingly predict the pressure variation when the flow reverses as well. Furthermore, when $K = \mathrm{Re}_{I,E} = \mathrm{Re}_{I,C} = 0$, the above equations reduce to the following forms for conventional heat pipes:

$$P^+_E = -8|\mathrm{Re}_{O,E}|\, z^{*2} - \frac{16}{3}\mathrm{Re}^2_{O,E}\, z^{*2} \tag{31}$$

$$P^+_A = -8z^* \tag{32}$$

$$P^+_C = 8\left(1 - \frac{2}{3}|\mathrm{Re}_{O,C}|\right)(|\mathrm{Re}_{O,C}|z^{*2} - z^*) \tag{33}$$

The above equations are in agreement with similar relations developed for conventional heat pipes (Busse, 1968).

## Conclusions

The results of the investigation warrant the following conclusions:

1 Equation (14) can be used to predict the sonic limit for the concentric annular heat pipe under symmetric and asymmetric heating loads.

2 Accurate estimates of the pressure loss in the evaporator section for compressible and incompressible vapor flows may be made by using equation (26).

3 An accurate prediction of the pressure loss can be made all along the concentric annular heat pipe by using the parabolic version of the equations of motion and solving for the pressure drops in the different segments of the heat pipe independently of each other. This can be done by assuming that the inlet axial velocity in the evaporator zone is zero and the axial velocity has a parabolic inlet profile for the adiabatic and condenser sections.

4 The hydrodynamic entry lengths for the evaporator, adiabatic, and condenser sections are very short and can be neglected in many practical applications. This justifies the usage of a similarity velocity profile along the length of the concentric annuluar heat pipe.

5 Accurate estimates of the pressure losses may be made by using equations (26), (28), and (30) for the evaporator, condenser, and adiabatic segments of the concentric annular heat pipe.

## Acknowledgments

Funding for this work was provided by the Thermal Energy Group of the Aero Propulsion Laboratory of the U.S. Air Force under contract No. F-33615-81-C-2012. The author is indebted to Dr. E. T. Mahefkey and Dr. J. E. Beam for their technical assistance during this project.

## References

Bankston, C. A., and Smith, H. J., 1973, "Vapor Flow in Cylindrical Heat Pipes," ASME JOURNAL OF HEAT TRANSFER, Vol. 95, pp. 371–376.

Busse, C. A., and Prenger, F. C., 1984, "Numerical Analysis of the Vapor Flow in Cylindrical Heat Pipes," in: *Research Development of Heat Pipe Technology*, Vol. I, pp. 214–219.

Busse, C. A., 1968, "Pressure Drop in the Vapor Phase of Long Heat Pipes," presented at the Thermionic Conversion Specialists Conference, Palo Alto, CA.

Deverall, J. E., Kemme, J. E., and Florschuetz, L. W., 1970, "Sonic Limitations and Start-Up Problems of Heat Pipes," Los Alamos Scientific Laboratory Rept. No. LA-4578.

Faghri, A., 1986, "Vapor Flow Analysis in a Double-Walled Concentric Heat Pipe," *Numerical Heat Transfer*, Vol. 10, No. 6, pp. 583–595.

Faghri, A., and Parvani, S., 1988, "Numerical Analysis of Laminar Flow in a Double-Walled Annular Heat Pipe," *Journal of Thermophysics and Heat Transfer*, Vol. 2, No. 2, pp. 165–171.

Kays, W. M., and Crawford, M., 1980, *Convective Heat and Mass Transfer*, McGraw-Hill, New York.

Kemme, J. E., 1969, "Ultimate Heat Pipe Performance," *IEEE Transaction on Electronic Devices*, Vol. ED-16, pp. 717–723.

Levy, E. K., 1968, "Theoretical Investigation of Heat Pipes Operating at Low Vapor Pressure," ASME *Journal of Engineering for Industry*, Vol. 90, No. 4, pp. 547–552.

Levy, E. K., 1971, "Effect of Friction on the Sonic Velocity Limit of Sodium Heat Pipes," presented at the AIAA 6th Thermophysics Conference, Tullhomer, TN.

Tien, C. L., and Rohani, A. R., 1974, "Analysis of the Effects of Vapor Pressure Drop on Heat Pipe Performance," *Int. Journal of Heat and Mass Transfer*, Vol. 17, pp. 61–67.

Vargaftik, N. B., 1975, *Handbook of Physical Properties of Liquids and Gases*, Hemisphere Publishing Corporation, Washington, DC.

Yuan, S. W., and Findelstein, A. B., 1955, "Laminar Flow With Injection and Suction Through a Porous Wall," *Proceedings of the Heat Transfer and Fluid Mechanics Institute*, Los Angeles, CA.